International Journal of Advances in Engineering and Management (IJAEM)
Volume 5, Issue 4 April 2023, pp: 1419-1424 www.ijaem.net ISSN: 2395-5252

Design and Fabrication of a Mechanical Bird (UAV)

Nidesh Chandan, Mihir Kubal, Aadya Limaye, Siddharth Pawar

Student, Datta Meghe College of Engineering, Airoli, Maharashtra
Student, Datta Meghe College of Engineering, Airoli, Maharashtra
Student, Datta Meghe College of Engineering, Airoli, Maharashtra
Student, Datta Meghe College of Engineering, Airoli, Maharashtra

Date of Submission: 15-04-2023 Date of Acceptance: 26-04-2023

ABSTRACT
This report is about the construction of an ornithopter which imitates the flapping motion of a bird's flight and the characteristics of lift and thrust generations of various wing designs are studied. This project focuses on the spar arrangement and the materials used for the wings that can achieve efficient performance. Different lift and thrust calculating methods are analyzed and evaluated. Different wing types of insects and birds were analyzed for understanding the production of lift created by the natural flyers by flapping the wings. Various experiments were conducted on different wing designs and materials and a design was developed for the spy eagle. The prototype comprises of a length of 100 cm and a wing span of 1.2 meters and weighs around 1300 grams. The mechanism which was to be used for the flapping motion of the wing was designed and fabricated. This was achieved with the use of a brushless motor and a flexible and light wing structure. The tail of the bird has a design concept like the elevators of an aircraft. The tail is divided into two parts controlled by 2 servo motors which can move in opposite directions or the same directions at the same time.

I. INTRODUCTION

We notice a growth in the need of miniature flight vehicles with improved capabilities like the micro air vehicles for military and civilian surveillance. The flapping wing concept of birds gives an example of utilizing unsteady aerodynamics to mechanize the miniature flight structures at low Reynolds numbers. This project attempts to mimic the flapping wing concept of natural flyers and analyze how lift is generated through this mechanism. The results achieved will be used to investigate the flow characteristics to improve the designs of ornithopters. The flapping concept is the avian type which is the vertical motion of the wings.

In this project, a resonance type flapping wing model is developed. This type of flapping wing utilizes the resonance phenomenon of a two degree of freedom elastic system i.e. springs are used to support the wings for flapping and feathering motions, oscillating, at a resonance frequency of the system. The amplitude of flapping and feathering motions and the phase angles between them can be controlled by varying the amount of damping.

EXPERIMENTATION:

<u>GEAR CALCULATIONS:</u>

Here, calculating the speed at which the wings will flap. For this the speed calculation at which each gear will be rotating which finally gives the speed for the flapping of the wings. The motor is a brushless DC motor 2020 3500 kv which means the motor has a speed of 3500 rpm / V. Since the being used is a 7.4 V 500 mAh battery, the speed of the motor will be:

Speed of the motor = 3500 / 7.4
= 25,900 rpm

<u>First Gear:</u>

Now, the first gear which is a pinion gear having 9 teeth will have the same speed as the motor since it's attached to the motor. Therefore,

Speed (1ST Gear) = 25,900 rpm

<u>Second Gear:</u>

For the second gear which is a spur gear having 70 teeth, the formula used to find the speed is:

Speed x No. of teeth = Speed x No. of teeth
(First gear) (Second gear)

25,900 x 9 = Speed (2ND Gear) x 70

Speed (2ND Gear) = (25900 x 9) / 70
Speed (2ND Gear) = 3330 rpm
Third Gear:
For the third gear which is a pinion wire having 9 teeth and will have the same speed as the second gear as it is attached to the second gear and will rotate at the same speed. Therefore,
Speed (3RD Gear) = 3330 rpm

Fourth Gear:
For the fourth gear which is a 70 teeth spur gear, the speed will be calculated using the same formula:
Speed x No. of teeth = Speed x No. of teeth
(Third gear) (Fourth gear)
3330 x 9 = Speed (4TH Gear) x 70
Speed (4TH Gear) = (3330 x 9) / 70
Speed (4TH Gear) = 428.143 rpm

	Pinion Gear	2nd Spur gear	Pinion wire	4th Spur Gear
Teeth (nos)	9	70	9	70
Module	1	1	1	1
Diameter (mm)	10	35	8	35
Width (mm)	6	6	6	6
Speed (rpm)	25,900	3,300	3,300	429

Table 1: Gear Calculations

Fuselage:
Fuselage head
Calculating the area for the head of the fuselage:

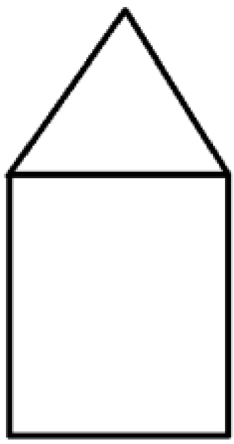

Area of a triangle = ½ x b x h
= ½ x 5 x 5
= 12.5 cm2
For the rectangle:
Area of rectangle = L x B
= 5.5 x 5
= 27.5 cm2
Total area of the part = 27.5 + 12.5
= 40 cm2

Now, considering the opposite side of the head also,
Total area = 40 x 2
= 80 cm^2

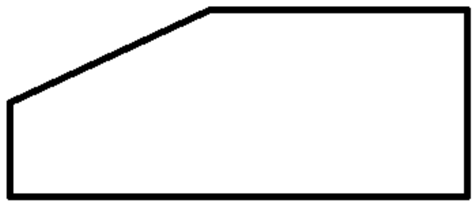

Calculating the area of the rectangle:
Area of the rectangle = L x B
= 10.5 x 1.5
= 15.75 cm^2
Calculating area of the trapezium:
Area of a Trapezium = ½ x (sum of the parallel sides) x breadth
= ½ x (10.5 + 7) x 5
= 43.75 cm^2
Total area of the part = 15.75 + 43.75
= 59.5 cm^2
Considering the opposite side of the part:
Total area = 59.5 x 2
= 119 cm2
Therefore, the total area of the head will be:
Total Area = 80 + 119
Total Area (HEAD) = 199 cm2
Calculating the area of the body of the fuselage:

6.3.2 Side:

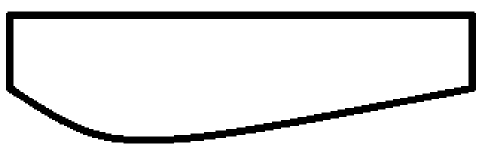

International Journal of Advances in Engineering and Management (IJAEM)
Volume 5, Issue 4 April 2023, pp: 1419-1424 www.ijaem.net ISSN: 2395-5252

Area of rectangle = L x B
= 10.4 x 4.7
= 48.88 cm2
Area of rectangle = 4 x 3.5
= 14 cm2

Area of rectangle = 6.1 x 2.8
= 17.08 cm2
Calculating total area of the side part of the fuselage:
Area = 48.88 + 14 + 17.08
= 79.96 cm2
Considering the opposite side of the fuselage body:
Total area = 79.96 x 2
Total Area (SIDE) = 159.92 cm2
Now, calculating the area for the top and bottom part of the fuselage:

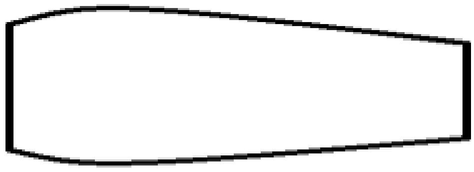

Area = 8.5 x 4.5
= 38.25 cm2
Area = 6.5 x 3.8
= 24.7 cm2

Area = 5.5 x 3
= 16.5 cm2
Calculating total area for the top part of the fuselage:
Area = 38.25 + 24.7 + 16.5
= 79.95 cm2

Considering the bottom part of the fuselage:
Total area = 79.95 x 2
Total Area (FUSELAGE BODY) = 158.9 cm2
Now, adding the area of the head and body of the fuselage to calculate the area of the total fuselage:
Total Area = 199 + 159.92 + 158.9
Total Area = 517.82 cm2
Total Area = 0.051782 m2
Parasitic Drag (CDP):

6.4.1 Wings:
CDP (WING) = (Cf x K x SWET) / SREF
SWET = 0.175 m2
SREF = 0.08742 m2
The value of ‘K’ is obtained from the table:
Thickness ratio = T / C = 0.1 / 0.6 = 0.167
From the table, the value of ‘K’ obtained is 1.125.
Cf = 1.328 / √RN

Reynolds Number (RN) = (V x l) / μ
Where, the estimated velocity is considered to be 7 m/s.
The viscosity ‘μ’ = 1.4607 x 10– 5
The length ‘l’ = mean aerodynamic chord (M.A.C)
M.A.C = (2/3) x CR x (1 + (
CT = 2 cm CR = 19 cm
M.A.C = (2/3) x 19 x (1 + 0.105 – (0.105 / (1 + 0.105)))
M.A.C = 12.79 cm = 0.128 m
RN = (7 x 0.128) / 1.4607 x 10– 5
RN = 61340.45
Cf = 1.328 / √61340.45 = 5.36 x 10– 3

Therefore,
CDP = ((5.36 x 10– 3) x 1.125 x 0.175) / 0.08742
CDP (WING) = 0.012
6.4.2 Tail:
CDP (WING) = (Cf x K x SWET) / SREF
CR = 19.5 cm
CT = 0.2 cm
M.A.C = (2/3) x 19.5 x (1 + 0.0103 – (0.0103 / (1 + 0.0103)))
M.A.C = 0.13 m
RN = (7 x 0.13) / 1.4607 x 10– 5
RN = 62298.9
Cf = 1.328 / √62298.9 = 5.32 x 10– 3
SWET = 0.034 m2
SREF = 0.01699 m2
CDP = ((5.32 x 10– 3) x 1.125 x 0.034) / 0.01699
CDP (TAIL) = 0.012

6.4.3 Fuselage:
CDP (WING) = (Cf x K x SWET) / SREF
SWET = 0.0325 m
SREF = 0.051782 m
The value of ‘K’ is obtained from the table:
Fineness ratio = L / D = 30.5 / 4.8 = 6.35
From the table, the value of ‘K’ is obtained to be 1.22.
RN = (7 x 0.305) / 1.4607 x 10– 5
RN = 146162.8
Cf = 1.328 / √146162.8
Cf = 3.47 x 10– 3
CDP = ((3.47 x 10– 3) x 1.22 x 0.0325) / 0.051782
CDP (FUSELAGE) = 2.657 x 10– 3
Now, adding up the parasitic drag for the wing, tail and the fuselage:
CDP (TOTAL) = 0.012 + 0.012 + (2.657 x 10– 3)
CDP (TOTAL) = 0.026657

6.5 Induced Drag (CDI):
CDI = CL2 / (π x AR x μ)
Aspect Ratio (AR) = b2 / S
= 1.042 / 0.175

International Journal of Advances in Engineering and Management (IJAEM)
Volume 5, Issue 4 April 2023, pp: 1419-1424 www.ijaem.net ISSN: 2395-5252

AR = 6.18
Assuming,
L = W
W = mg
= 0.170 x 9.81
W = 1.67 N
Therefore,
L = 1.67 N
L = ½ ρ V2 S CL
CL = L / (½ ρ V2 S)
CL = 1.67 / (½ x 1.225 x 72 x 0.175)
CL = 0.32
Therefore,
CDI = 0.322 / (π x 6.18 x 0.98)
For non-swept back wings (u = 0.98)
CDI = 5.382 x 10– 3
Now,
CD = CDP + CDI
= 0.026657 + (5.382 x 10– 3)
CD = 0.032039
D = ½ ρ V2 S CD
= ½ x 1.225 x 72 x 0.175 x 0.032039
Drag = 0.1683 N
Lift to Drag ratio:
L / D = 1.67 / 0.168
L / D = 9.94

Therefore, the total lift to drag ratio experienced by the bird is 9.94.
OBSERVATION:

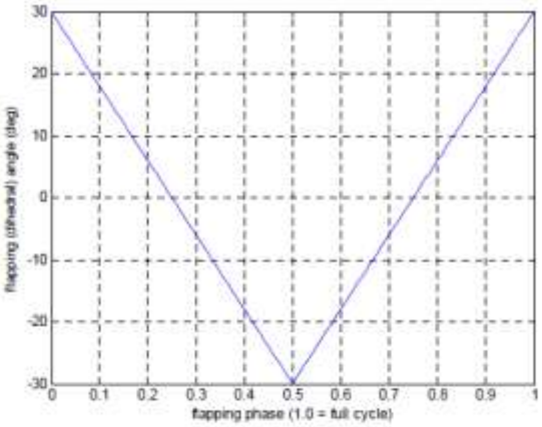

Graph 1 : Flapping Pattern

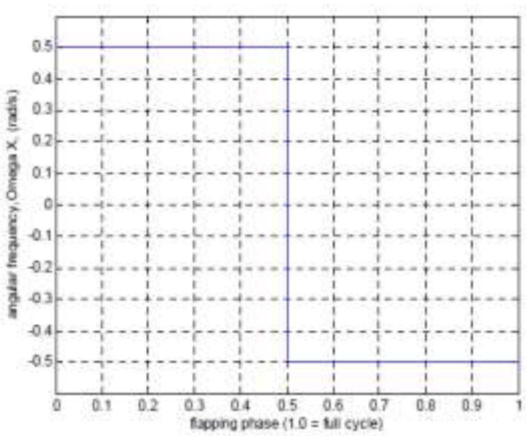

Graph 2: Angular Velocity for Flapping angle

At the start, the position of the wing was kept at + 30o degree dihedral angle. When the wings began to flap, the wing flapped downwards about its chord. At the outer half of the wing the flow separated from the wing, which causes a vortex to form which is visible at the top. There is a flow separation at the trailing edge, near the root at the area close to the scapula. This results in the formation of strong leading edge vortex producing high lift at the initial start of the down stroke motion.

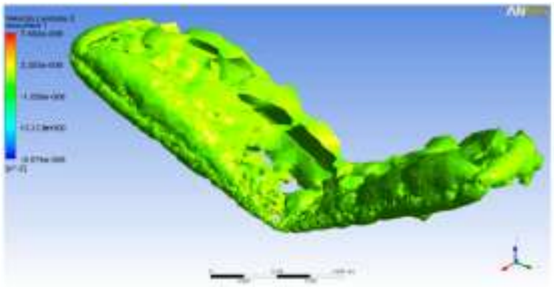

Figure 11: Structure of Vortex on the wing

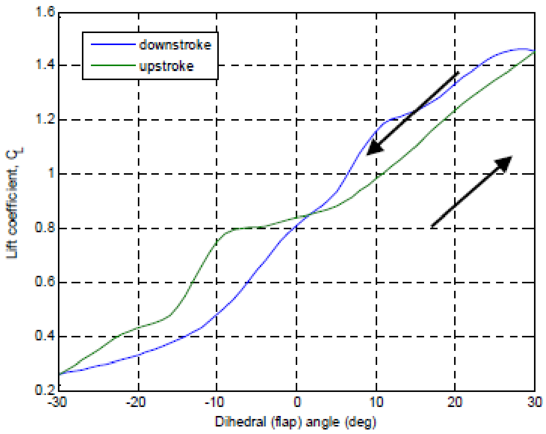

Graph 3: Lift co-efficient for down stroke and upstroke of the wing.

International Journal of Advances in Engineering and Management (IJAEM)
Volume 5, Issue 4 April 2023, pp: 1419-1424 www.ijaem.net ISSN: 2395-5252

With time, the flow keeps separating across the wing, which forms the strong leading-edge vortex over the wing. At the inboard area close to the trailing edge and scapula, the wake is more dominant. There is more lift generated through the push down motion of the wing. Post midpoint, the vortex tends to increase, and the flow separates from the entire wing at the leading edge close to the alula. The wake near the trailing edge of the wing also separates into outer and inner parts. The graph above determines the lift coefficient for down stroke and upstroke motions of the wing.

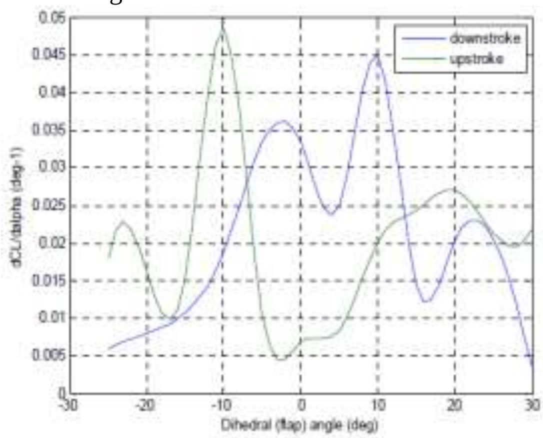

Graph 4: Lift co-efficient derivative corresponding to flapping angles

The graph above determines the lift coefficients derivatives for the flapping angles which is essential for the dynamics of flight and control.

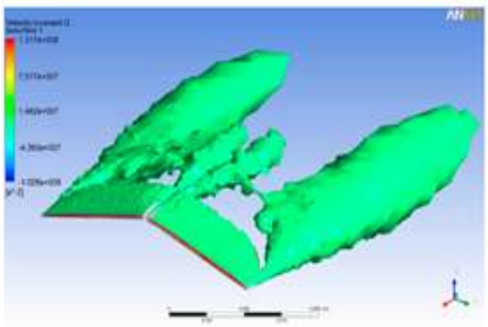

Figure 22: Vorticity over the wing

The figure above determines the structure of the vortex when the wings are at an angle of – 15o. The vortex on the leading edge appears to be more dominant as it covers the wing entirely. The wingtip vortices can be seen clearly with the wake present behind the wing.

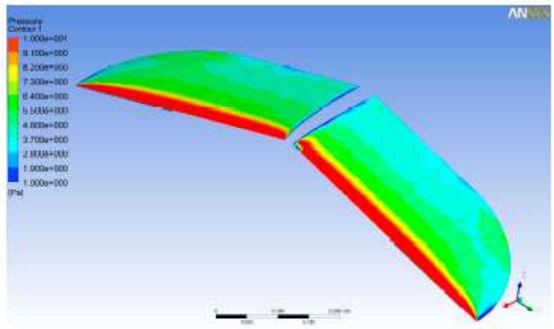

Figure 3: Surface pressure (TOP)

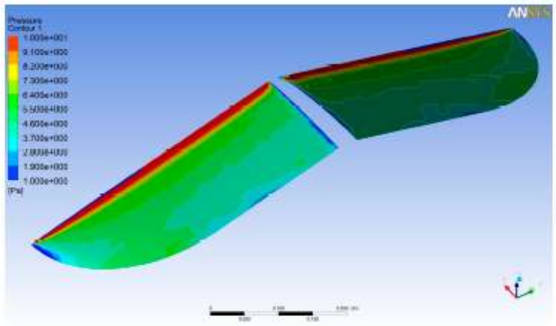

Figure 4: Surface pressure (BOTTOM)

The two figures above show the pressure on the surface of the spy eagle's wing when the angle of the wings are – 15o. A region of low pressure can be seen at the tip which can be seen colored in blue. Therefore, we can say that the bird maneuvers through flapping whole wingspan at varied amplitudes instead of using its wing tip only.

These results that show unsteady flow determines that the bird produces lift on the wings through vortex lift mechanism. Lift is produced through flapping the entire wings at varied amplitudes instead of using the wing tip only. Addition of span wise flapping may tune the position inflight.

II. CONCLUSION:

This report carries out a research and development on the Mechanical Bird which is a flapping wing UAV. The UAV mimics other flying birds. Results suggest that the Bird creates lift by the vortex lift mechanism. They maneuver by the flapping motion of their wings at varied amplitudes rather than using the wingtip only. In a forward motion, the wings generate a vortex ring at the leading edge. The performance of the ornithopter is analyzed through calculations done to calculate the lift, drag, maneuver, and center of gravity and these are used for predicting the flying performance of the ornithopter. While measuring the aerodynamic forces, it was noticed that there was constant generation of thrust, while the lift was periodic in nature followed by a sinusoidal trend. It was noticed that there was lift generated mostly during the down stroke with negative lift being created during the upstroke. Flexible wings tend to produce high velocity, higher frequency, lift and thrust. While analyzing the wing angle motion, it was noticed that there was positive lift produced when the wing was at an angle of 0o and – 10o and there was negative lift produced when the wing was at an angle of 30o and 45o.

SOME OF THE ADVANTAGES FROM THE ABOVE RESULTS
An ornithopter could have near vertical take offs
The agile dynamic maneuvers of birds could outperform those of aircraft and allow for better surveillance and use in hostile environments.
Ornithopters can fly at low speeds
The gliding process and lower start time of the flapping compared to jet and propeller engines allows for a real glide as opposed to cruise conditions obtained by jet aircrafts.

REFERENCES:

[1]. U. M. Norberg, Vertebrate Flight vol. 27. New York: Springer-Verlag, 1990.
[2]. W. Bejgerowski, J. W. Gerdes, H. A. Bruck, S. K. Gupta, "Design and fabrication of miniature compliant hinges for multi-material compliant mechanisms," International Journal of Advanced Manufacturing Technology, vol. 57, pp. 437-452, 2011.
[3]. SmartBird. Festo Corporate. (n.d.). Retrieved April 25, 2016
[4]. Beando, A., Chung, J., Overton, C., Pietri, T., & Ramirez, K. (2014). Theoretical Model and Test Bed for the Development and Validation of Ornithopter Designs. Worcester Polytechnic Institute. Retrieved September 21, 2015.
[5]. Woei-Leong Chan, ―Ornithopter Type Flapping Wings for Autonomous Micro Air Vehicles‖, Aerospace, 13 May 2015.
[6]. Dr. Ankur Geete, ―CFD Analysis of Conceptual Aircraft Body, International Research Journal of Engineering and Technology, 01 January 2017.
[7]. HarijonoDjojodihardjo, ―Two-Dimensional CFD Simulation For Visualization of Flapping Wing Ornithopter Studies, Arpn Journal Of Engineering and Applied Sciences, November 2015.